Asociación Argentina
de Mecánica Computacional

Mecánica Computacional Vol XXX, págs. 1239-1256 (artículo completo)
Oscar Möller, Javier W. Signorelli, Mario A. Storti (Eds.)
Rosario, Argentina, 1-4 Noviembre 2011

ON THE INFLUENCE OF THE SHAPE OF WINDOWS ON OVERPRESSURES AND IMPULSES IN BUILDINGS SUBJECTED TO EXTERNAL BLAST LOADING

Abel Montoro[a,b] and Daniel Ambrosini[a,b]

[a]*Maestría en Ingeniería Estructural, Facultad de Ingeniería, Universidad Nacional de Cuyo Centro Universitario - Parque Gral. San Martín - 5500 Mendoza, dambrosini@uncu.edu.ar*
http://fing.uncu.edu.ar/academico/posgrados/estructural/maestria-en-ingenieria-estructural
[b]*CONICET*

Keywords: Blast loading, Structural design, Opening, Hydrocodes.

Abstract. Explosive charges have attracted considerable attention in recent years due to accidental or intentional events involving important structures which have occurred around the world. The activities related to terrorist attacks have increased and, unfortunately, the current trend suggests that they will continue to rise in the future. In relation to the design of structures subjected to blasts there are still many uncertainties in the specialized technical literature. Moreover, many studies done in different countries remain as “classified” documents which can not be accessed by foreign researchers. The main objective of this work is to formulate design recommendations concerning the shape of openings and windows in structures that may be subjected to blasts. With this purpose, numerical studies of a typical building subjected to external blast loadings of 50, and 500 kg of TNT located at different stand-off distances were carried out. Using a hydrocode, the multiple reflections of the pressure wave generated by the explosion, the "Mach effect”, the rarefactions, and the negative phase of the incident pressure wave can be accurately reproduced. The pressure and impulse histories at various points inside the structure caused by the external loads were also determined. Finally, shapes of windows to mitigate the effects of external blast loadings on buildings are recommended.

1 INTRODUCTION

In general, structural, mechanical systems and civil structures are not designed to resist dynamic loads of short duration and high amplitude. At present, consideration of blast loading due to a terrorist attack is mainly restricted to special structures such as military structures, nuclear power plants, embassies, etc.

Unfortunately, the 1993 and 2001 attacks on the World Trade Center in New York, as well as examples in our country and elsewhere, clearly demonstrate that it is necessary to consider loads from deliberate attacks. However, it is noteworthy that the origin of the impulsive charges can not only be always from attacks. There are several types of impulsive loadings which can cause similar damage, e.g. military or industrial explosions, accidental explosions in petrochemical plants, aircraft or vehicle impact or impact of waves on marine structures. These cases illustrate the need of technical information to improve the structural safety for both military and civilian structures.

Historically, research about explosions has been carried out predominantly using simplified analytical methods (Baker et al. 1983, Kinney and Graham 1985, Smith et al 1994) or required the use of supercomputers for detailed numerical simulations. In recent decades, with the development of computer hardware is being possible carry out detailed numerical simulations on PCs, which has greatly increased the ability of these methods. The development of integrated hydrocodes, complete the set of tools necessary to carry out successfully numerical analysis. Major issues such as the multiple reflections of the pressure wave generated by the explosion, the "mach" effect, rarefactions and the negative phase of the pressure wave can be accurately reproduced by explicit dynamic computer programs. Simplified and semi empirical analytical techniques normally ignore these phenomena and can not be used for the evaluation of pressures and impulses in such scenarios (Smith and Rose 2002)

In the specialized literature, there are studies related to the calibration of models, such as the correct representation of the blast load and the high nonlinearity of the materials (Shunfeng et. al. 2009). Moreover, theoretical-numerical-experimental analysis of the response of different structural components under explosive loading is founded, mainly on steel plates (Jacinto et. al. 2001, Jacob et al. 2007), slabs and concrete columns (Jones et al. 2009, Luccioni and Luege 2006, Schenker et al. 2008, Shi et al. 2008), concrete structures (Yang and Lok 2007, Lu and Xu 2007), lattice structures (McKown et al. 2008), and suspended roofs (Raftoyiannis et al. 2007). The study of the dynamic response with protective barriers of the pressure waves generated by explosions is attracted growing interest in recent years (Coughlin et al. 2010, Remennikov et al. 2007, Zhou and Hao 2008, Ambrosini and Luccioni 2009). As a protection structure Borvik et al. (2008a and b) presented a experimental-numerical study of a container and metal structures and Scherbatiuk et al. (2008) used soil-filled walls. The development of structural components of protection has been extremely active in recent times, both for sandwich panels (Dharmasena et al. 2010, Main and Gazonas 2008, Tekalur et al. 2008) and the use of composite materials (Batra and Hassan 2008). Finally, Esper (2003) presents an analysis of buildings damage under explosive charges and recommendations for protective measures.

The main objective of this paper is to determine the influence of the shape of windows on the dynamic response of structures subjected to blasts. A hydrocode (AUTODYN 3D) is used for this purpose. A typical building subjected to external explosions of 50 and 500 Kg. of TNT placed at different distances from it was studied. An analysis of pressures and impulses is performed at various control points located inside the structure under study, taking into account the multiple reflections of the pressure wave produced on the floor and walls.

2 DESCRIPTION OF THE PROBLEM

2.1 Scenario

A simple environment is discussed in this paper as shown in Figure 1: A building with rigid walls of 10x10m in plan, 4.0m height and one opening at the facade. The air in which is embedded the building under study has different dimensions depending on the masses of explosive and the distances at which they are located. For this reason, the models will be larger when the mass of explosive and the distance of the focus of the explosion are larger.

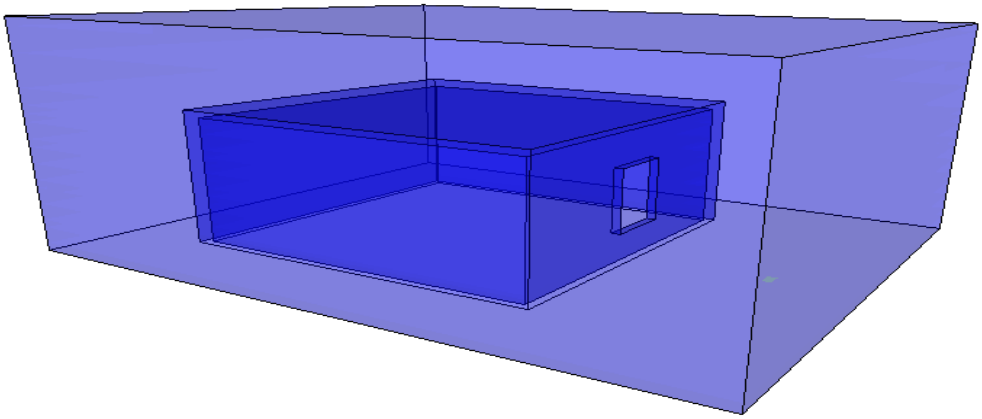

Figure 1: Environment under consideration

2.2 Alternatives analyzed

Explosive mass: In order to obtain comparable results, the mass of explosive is defined by kg of TNT. The masses for other types of explosive can be obtained with the concept of TNT equivalency (Wharton et al. 2000). 50 and 500 kg of TNT were used because these charges are in the middle range used in terrorist attacks. The mass range of explosive used in terrorist attacks is discussed in some studies (Elliot et al. 1992, Ambrosini and Luccioni 2010) and it is strongly dependent on the transport of the explosive.

Focus location: Four locations of the explosion focus were considered for each of the explosive masses, considering four different scaled distances, previously established as shown in Tables 1 and 2.

Windows size: Three options were considered, whose dimensions are shown in Table 3 and Figure 2. In all alternatives, the area of the opening is approximately 10% of the total area of the facade.

Table 1: Focus of the explosion for 50 kg of TNT

Mass of TNT = 50 kg	
Scaled distance [m/kg$_{TNT}^{1/3}$]	**Focus location [m]**
0,50	1,84
1,00	3,68
2,00	7,37
3,00	11,05

Table 2: Focus of the explosion for 500 kg of TNT

Mass of TNT = 500 kg	
Scaled distance [m/kg$_{TNT}^{1/3}$]	**Focus location [m]**
0,50	3,97
1,00	7,94
2,00	15,87
3,00	23,81

Table 3: Size of the windows

Alternative	**Dimensions**		**Area covered [%]**
	Width [m]	**Hight [m]**	
1	2,00	2,00	10,00
2	4,00	1,00	10,00
3	1,00	4,00	10,00
4	3,25	1,25	10,15
5	1,25	3,25	10,15

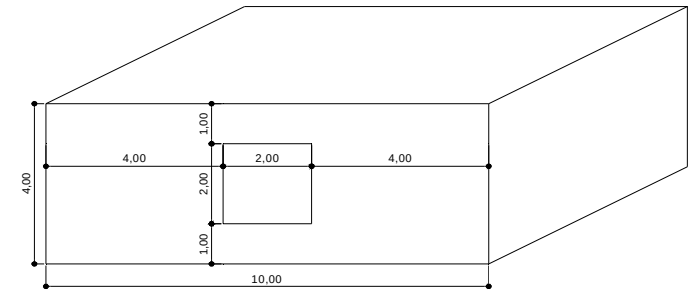

(a)

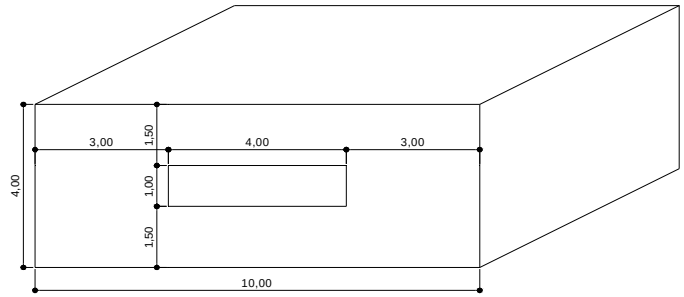

(b)

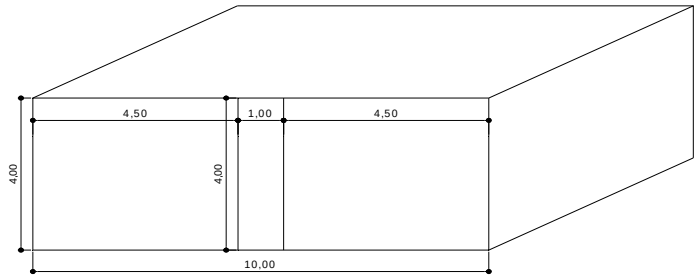

(c)

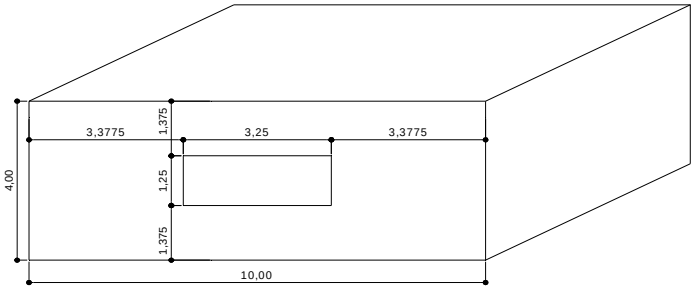

(d)

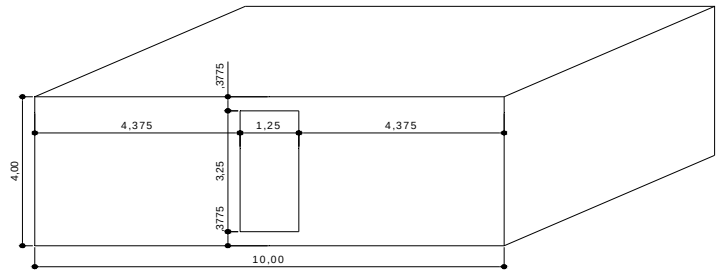

(e)

Figure 2: Window options (a) Alternative 1 (b) Alternative 2 (c) Alternative 3 (d) Alternative 4 (e) Alternative 5

3 GENERATION OF BLAST LOADING

The use of symmetry conditions allows the spherical portion of the blast wave expansion to be represented by a spherical model. This is achieved by a one-dimensional (1D) mesh using spherical symmetry. The number of cells required to produce accurate solutions is greatly reduced when compared with a full 3D model. When the spherical blast wave begins to interact with obstacles, the flow becomes multi-dimensional. However, before this time, the 1D solution can be imposed or remapped onto a specific region of the multi-dimensional model. The 3D calculation can then proceed from that point. This reduces the required time for the calculation and increases the accuracy due to the fine resolution of the 1D mesh in the initial stage of detonation and expansion.

3.1 Detonation and initial expansion

According to the mentioned above, the problem under study is divided into two stages: a) initial detonation and expansion b) blast propagation. The initial detonation and expansion of the sphere of high explosive were modeled in a 1D, spherically symmetric model of 1 m radius. It was estimated that the center of the explosive is located at 1.00 m from the floor.

The 1D expansion analysis continued until just prior to impingement of the blast wave on the rigid surface. At this time a 1D remap file was created and then imported into a three-dimensional model, allowing the reflection of the blast wave off the ground and walls to be modeled. 1D models are presented in Figure 3 where it is raised for each mass of explosive twice the number of elements that the minimum number that the documentation recommends to avoid numerical problems. Table 4 shows the different radios for each spherical charge in function of the TNT density.

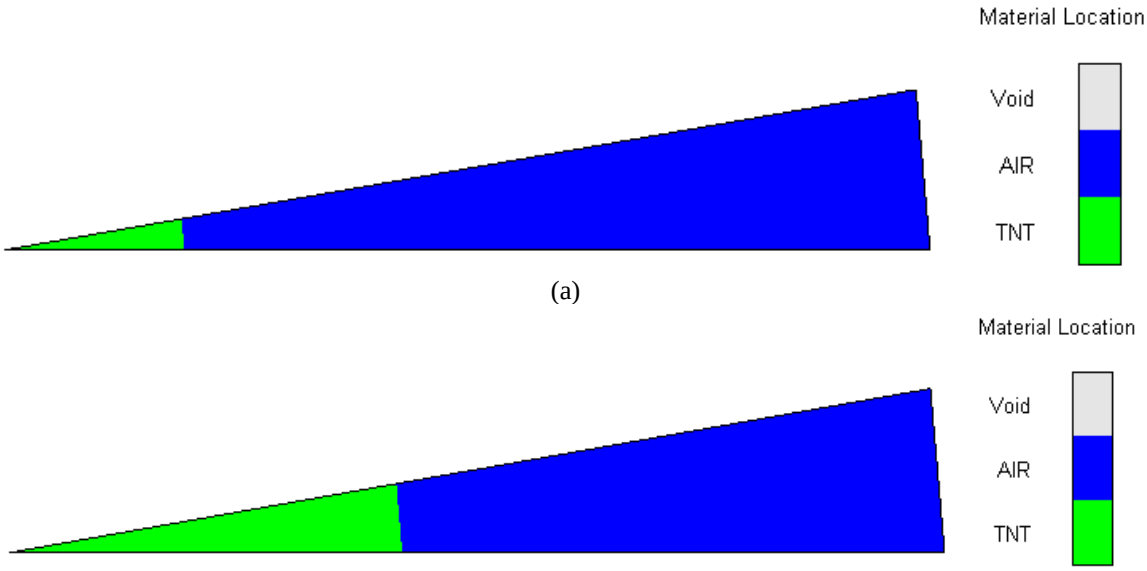

Figure 3: 1D model. (a) 50 Kg TNT. (b) 500 Kg TNT

Table 4: Radius of the spherical charges

TNT masse [kg]	Radius of the spherical charges [cm]
50	19,42
500	41,84

4 NUMERICAL MODEL

4.1 Materials models

a) Air: The ideal gas equation of state was used for the air. This is one of the simplest forms of equation of state for gases. In an ideal gas, the internal energy is a function of the temperature alone and if the gas is polytropic the internal energy is simply proportional to temperature. It follows that the equation of state for a gas, which has uniform initial conditions, may be written as,

$$p = (\gamma - 1)\rho e \tag{1}$$

in which p is the hydrostatic pressure, ρ is the density and e is the specific internal energy. γ is the adiabatic exponent**,** it is a constant (equal to $1 + R/c_v$) where constant R may be taken to be the universal gas constant R_0 divided by the effective molecular weight of the particular gas and c_v is the specific heat at constant volume.

b) TNT: High explosives are chemical substances which, when subject to suitable stimuli, react chemically very rapidly (in order of microseconds) releasing energy. In the hydrodynamic theory of detonation, this very rapid time interval is shrunk to zero and a detonation wave is assumed to be a discontinuity which propagates through the unreacted material instantaneously liberating energy and transforming the explosive into detonating products. The normal Rankine-Hugoniot relations, expressing the conservation of mass, momentum and energy across the discontinuity may be used to relate the hydrodynamic variables across the reaction zone. The only difference between the Rankine-Hugoniot equations for a shock wave in a chemically inert material and those for a detonation wave is the inclusion of a chemical energy term in the energy conservation equation.

Since the 1939-45 war, when there was naturally extensive study of the behaviour of high explosives, there has been a continuous attempt to understand the detonation process and the performance of the detonation products, leading to considerable improvements in the equation of state of the products. The most comprehensive form of equation of state developed over this period, the “Jones - Wilkins - Lee” (JWL) equation of state, is used in this paper.

$$p = C_1\left(1 - \frac{\omega}{r_1 v}\right)e^{-r_1 v} + C_2\left(1 - \frac{\omega}{r_2 v}\right)e^{-r_2 v} + \frac{\omega e}{v} \tag{2}$$

Where $v = 1/\rho$ is the specific volume, C_1, r_1, C_2, r_2 and ω (adiabatic constant) are constants and their values have been determined from dynamic experiments and are available in the literature for many common explosives.

It can be shown that at large expansion ratios the first and second terms on the right hand side of Equation (2) become negligible and hence the behaviour of the explosive tends towards that of an ideal gas. Therefore, at large expansion ratios, where the explosive has expanded by a factor of approximately 10 from its original volume, it is valid to switch the equation of state for a high explosive from JWL to ideal gas. In such a case the adiabatic exponent for the ideal gas, γ, is related to the adiabatic constant of the explosive, ω, by the relation $\gamma=\omega+1$. The reference density for the explosive can then be modified and the material compression will be reset. Potential numerical difficulties are therefore avoided.

An explosion may be initiated by various methods. However, whether an explosive is dropped, thermally irradiated or shocked, either mechanically or from a shock from an initiator (of more sensitive explosive), initiation of an explosive always goes through a stage

in which a shock wave is an important feature. Lee-Tarver equation of state (Lee and Tarver 1980) was used to model both the detonation and expansion of TNT in conjunction with JWL EOS to model the unreacted explosive.

4.2 Analyzed models

In the analyzed models arise different environment sizes in front of the building facade according to the distances from the explosive source and amount of explosive. The number of elements involved in the models varies between 136.192 and 678.400 (Figure 4).

After considering various alternatives, taking into account other analyzes (Luccioni et al. 2006) was adopted as a measure of cubic elements 0.25 m, which is a measure that give a compromise between the precision of the solution and the computational cost. The model is solved by Euler formulation in which the nodes are fixed and the material (air) flows through the elements. Walls and the roof of the building are defined as regions "unused" and are considered as rigid surfaces. A boundary condition "flow-out" is defined at the boundaries of the models which is a transmitter edge that allows the pressure wave passes through the boundary without being reflected.

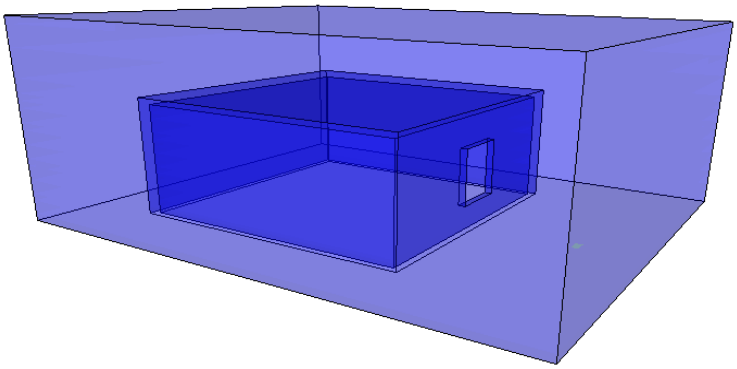

(a)

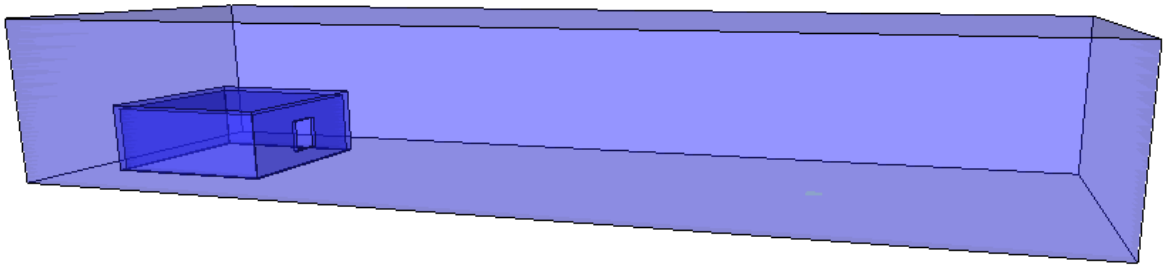

(b)

Figure 4: 3D model. (a) 136.192 elements. (b) 678.400 elements.

4.3 Checkpoints (Gauges)

In order to analyze the pressures and impulses generated inside the building several checkpoints are defined in the model, arranged as shown in Figure 5. These points are distributed on the near of all walls and some located within the room. In each of these points are stored all the variables of interest.

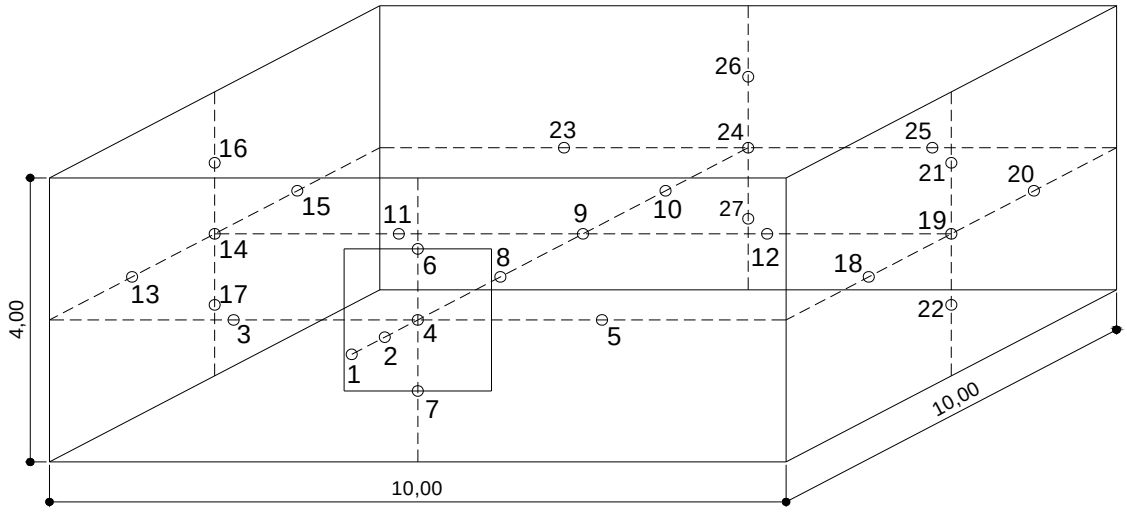

Figure 5: Checkpoints in the models.

5 RESULTS AND DISCUSSION

5.1 Blast wave propagation

For space reasons, at this point, the results for one of the alternatives analyzed are presented. In particular, the case presented is the alternative 2 with a blast load of 50 kg of TNT located at 1,842 m (z = 0.50 m/kgTNT$^{1/3}$) of the facade (see Tables 1 and 3).

Figure 6 shows the propagation of pressure wave in front of the building, and its penetration through the window hitting the floor and inner side walls, to make contact with the back wall. The multiple reflections that occur inside the building and the ground lead to a complicated and completely irregular pressures flow.

In this case, in which both the charge and the window are centered on the midpoint of the environment under consideration, obviously there is symmetry of the pressure wave from the axis through it.

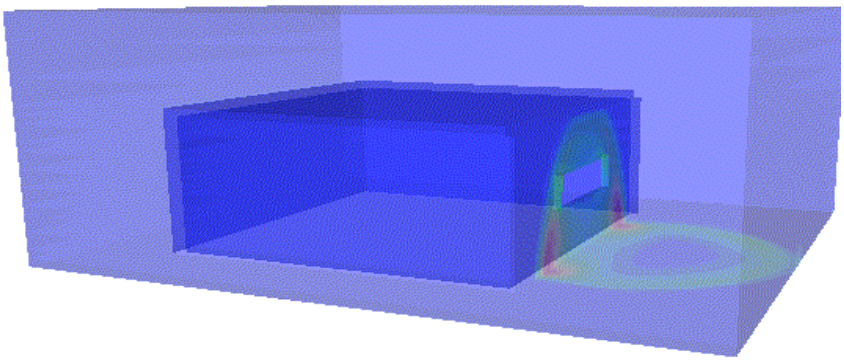

(a)

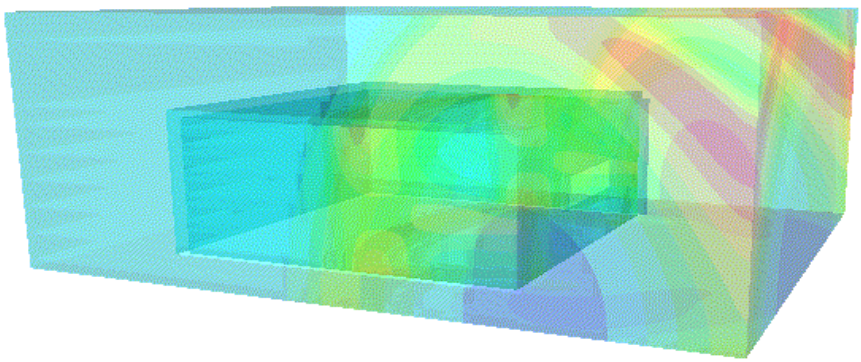

(b)

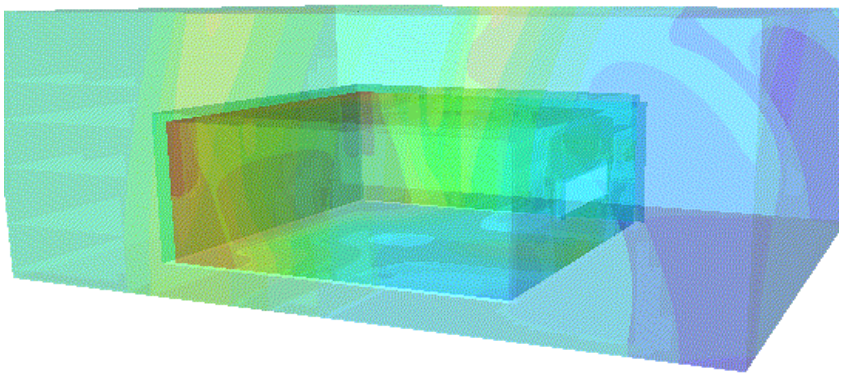

(c)

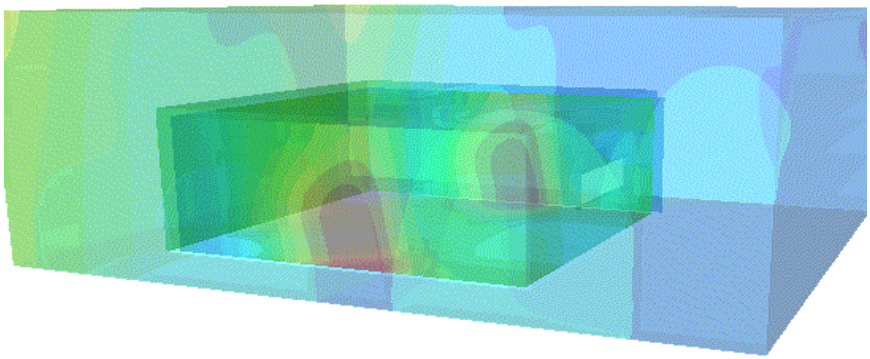

(d)

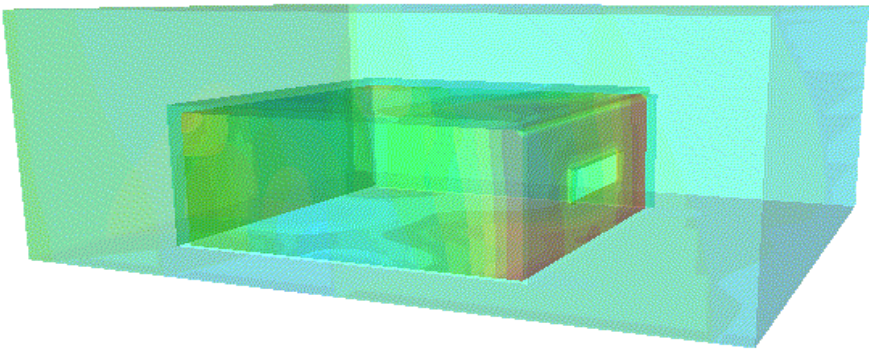

(e)

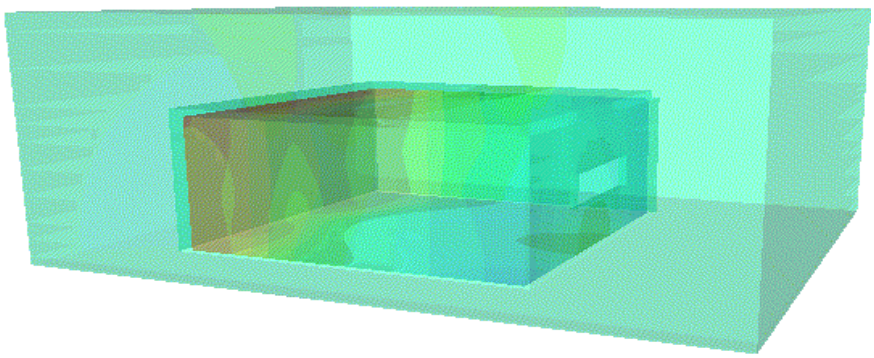

(f)

Figure 6: Pressure wave propagation.
(a) 1.819 ms. (b) 12.88 ms. (c) 23.19 ms. (d) 38.73 ms. (e) 78.84 ms. (f) 79.57 ms.

5.2 Pressures and impulses inside the building

According to that mentioned in Section 4.3, all variables of interest are stored in the checkpoints. This is a large volume of data that must be carefully evaluated and analyzed. From the standpoint of the paper objectives, there are two variables that are of particular interest: Pressures and the associated impulses.

In the tables 5 to 14 it can be seen the values recorded in the checkpoints that were taken as reference for comparative analysis of the different alternatives proposed. For space reasons only the results for a mass of 50 kg of TNT are presented, but these results are qualitatively similar that for the case of 500 kg of TNT.

Table 5: Maximum pressures for alternative 1

	Maximum Pressures [kPa]			
Gauges	**z = 0.50 m/kg$^{1/3}$**	**z = 1.00 m/kg$^{1/3}$**	**z = 2.00 m/kg$^{1/3}$**	**z = 3.00 m/kg$^{1/3}$**
4	830,90	476,12	232,83	161,61
9	150,31	130,94	117,29	111,18
14	187,90	153,98	127,74	116,92
24	168,33	143,37	122,73	113,81

Table 6: Maximum impulses for alternative 1

	Maximum Impulses [kPa ms]			
Gauges	**z= 0.50 m/kg$^{1/3}$**	**z= 1.00 m/kg$^{1/3}$**	**z= 2.00 m/kg$^{1/3}$**	**z= 3.00 m/kg$^{1/3}$**
4	1091,30	675,12	456,01	298,50
9	303,88	958,68	295,03	202,36
14	364,13	987,67	297,69	208,52
24	521,73	1272,9	405,15	294,57

Table 7: Maximum pressures for alternative 2

	Maximum Pressures [kPa]			
Gauges	**z = 0.50 m/kg$^{1/3}$**	**z = 1.00 m/kg$^{1/3}$**	**z= 2.00 m/kg$^{1/3}$**	**z= 3.00 m/kg$^{1/3}$**
4	796,10	419,66	215,71	153,90
9	138,18	219,14	117,81	111,49
14	163,18	283,56	124,06	114,93
24	160,54	427,74	124,37	113,85

Table 8: Maximum impulses for alternative 2

	Maximum Impulses [kPa ms]			
Gauges	**Z = 0.50 m/kg$^{1/3}$**	**Z = 1.00 m/kg$^{1/3}$**	**Z = 2.00 m/kg$^{1/3}$**	**Z = 3.00 m/kg$^{1/3}$**
4	855,62	479,03	340,39	230,58
9	849,74	219,14	323,38	207,09
14	878,38	283,56	319,91	213,30
24	1119,6	427,74	426,81	298,55

Table 9: Maximum pressures for alternative 3

	Maximum Pressures [kPa]			
Gauges	**Z = 0.50 m/kg$^{1/3}$**	**Z = 1.00 m/kg$^{1/3}$**	**Z = 2.00 m/kg$^{1/3}$**	**Z = 3.00 m/kg$^{1/3}$**
4	875,96	489,77	231,64	156,38
9	180,03	139,04	118,79	112,09
14	188,25	153,41	128,25	117,37
24	170,87	141,68	122,11	115,13

Table 10: Maximum impulses for alternative 3

	Maximum Impulses [kPa ms]			
Gauges	**z= 0.50 m/kg$^{1/3}$**	**z= 1.00 m/kg$^{1/3}$**	**z= 2.00 m/kg$^{1/3}$**	**z= 3.00 m/kg$^{1/3}$**
4	779,04	639,49	347,86	210,5
9	590,06	263,11	132,31	89,72
14	616,21	337,29	153,83	103,41
24	980,72	512,81	277,14	192,19

Table 11: Maximum pressures for alternative 4

	Maximum Pressures [kPa]			
Gauges	**z = 0.50 m/kg$^{1/3}$**	**z = 1.00 m/kg$^{1/3}$**	**z = 2.00 m/kg$^{1/3}$**	**z = 3.00 m/kg$^{1/3}$**
4	795,80	413,51	213,44	152,45
9	142,71	130,26	118,85	112,57
14	165,41	144,18	126,18	116,55
24	164,68	145,80	125,20	115,56

Table 12: Maximum impulses for alternative 4

	Maximum Impulses [kPa ms]			
Gauges	**z= 0.50 m/kg$^{1/3}$**	**z= 1.00 m/kg$^{1/3}$**	**z= 2.00 m/kg$^{1/3}$**	**z= 3.00 m/kg$^{1/3}$**
4	589,07	443,03	292,03	210,2
9	318,08	214,22	128,87	89,28
14	434,98	279,51	152,49	108,26
24	702,59	446,62	276,73	199,67

Table 13: Maximum pressures for alternative 5

	Maximum Pressures [kPa]			
Gauges	**z = 0.50 m/kg$^{1/3}$**	**z = 1.00 m/kg$^{1/3}$**	**z = 2.00 m/kg$^{1/3}$**	**z = 3.00 m/kg$^{1/3}$**
4	850,43	511,87	238,06	160,65
9	158,73	134,34	118,81	112,04
14	202,80	159,97	129,73	117,95
24	169,23	142,88	122,07	114,78

Table 14: Maximum impulses for alternative 5

	Maximum Impulses [kPa ms]			
Gauges	**z= 0.50 m/kg$^{1/3}$**	**z= 1.00 m/kg$^{1/3}$**	**z= 2.00 m/kg$^{1/3}$**	**z= 3.00 m/kg$^{1/3}$**
4	827,27	704,12	395,53	241,23
9	472,74	249,54	132,25	89,97
14	511,41	312,90	153,12	104,77
24	834,27	490,59	276,23	192,83

Figures 7 to 11 show time histories of pressures and impulses in gauge 24, corresponding to the detonation of a mass of 50 kg of TNT for the five alternatives proposed, with scaled distance of 0.50 m/kg$^{1/3}$.

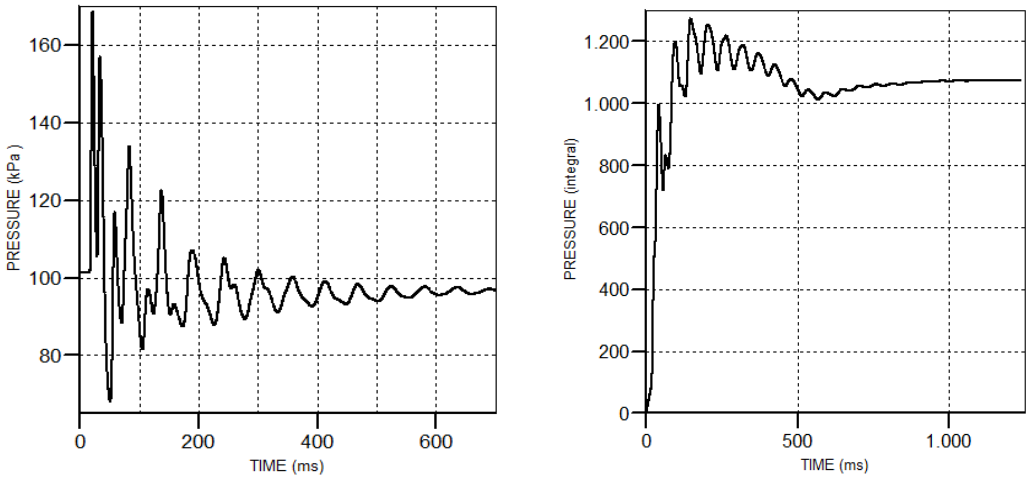

(a) (b)

Figure 7: Time histories. Alternative 1. (a) Pressures. (b) Impulses

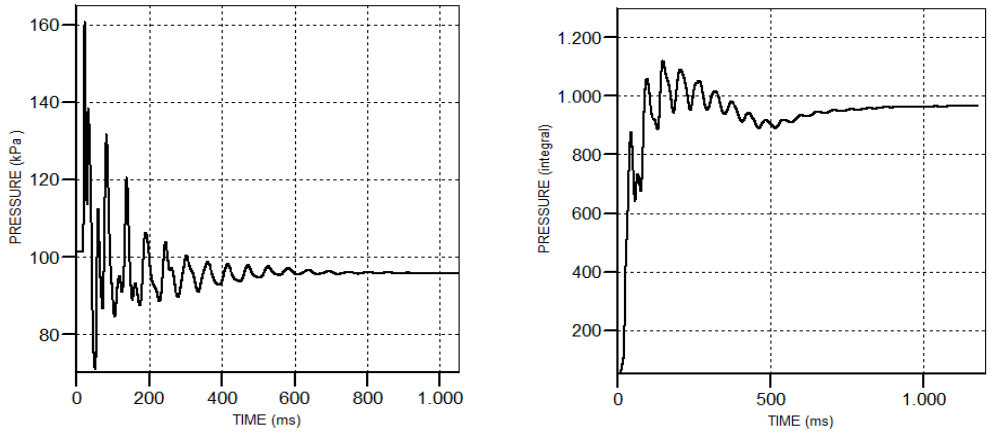

(a) (b)

Figure 8: Time histories. Alternative 2. (a) Pressures. (b) Impulses

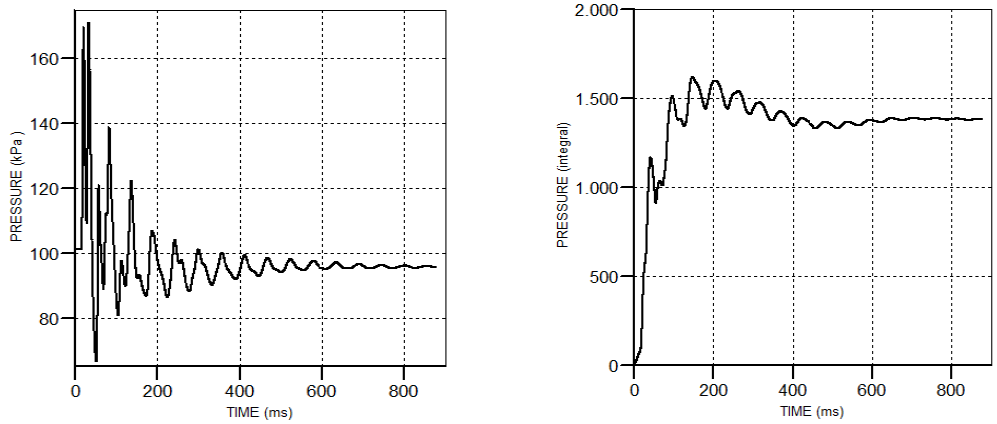

(a) (b)

Figure 9: Time histories. Alternative 3. (a) Pressures. (b) Impulses

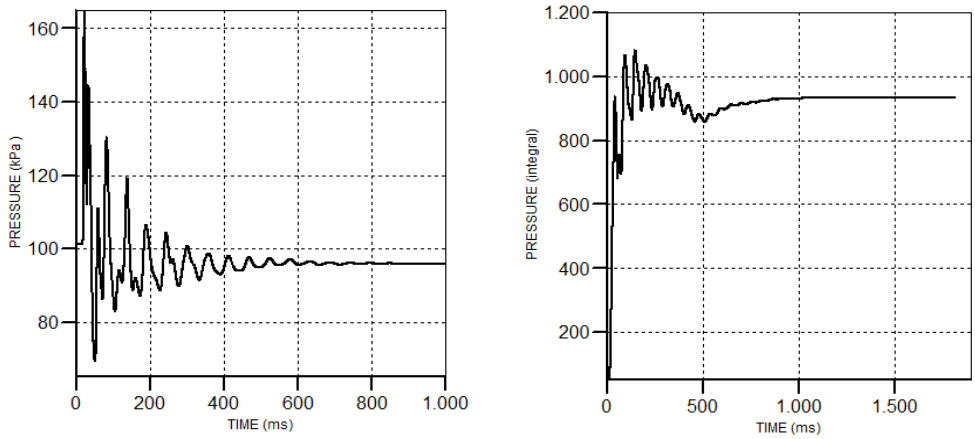

(a) (b)

Figure 10: Time histories. Alternative 4. (a) Pressures. (b) Impulses

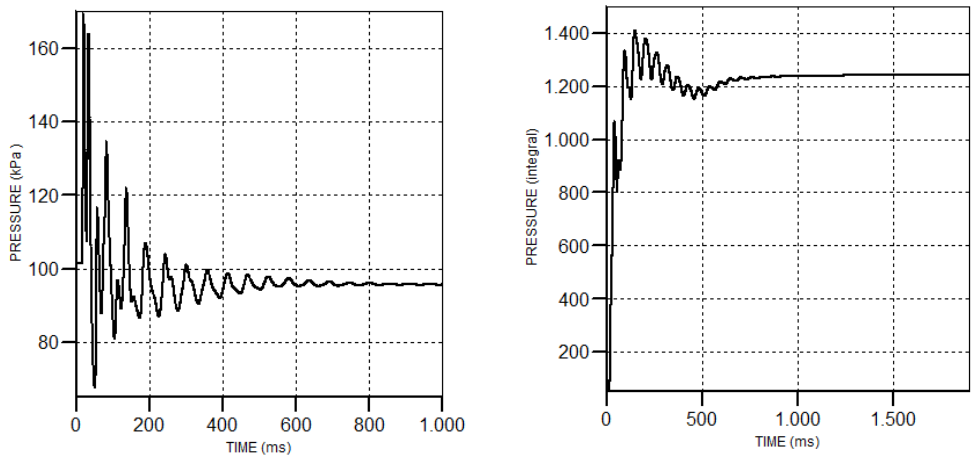

(a) (b)

Figure 11: Time histories. Alternative 5. (a) Pressures. (b) Impulses

Figures 12 to 15 show a comparison of the peak pressure and impulse values from the explosion caused by a mass of 50 and 500 kg of TNT, respectively, for the available alternatives analyzed, in checkpoints 4, 9, 14, 24.

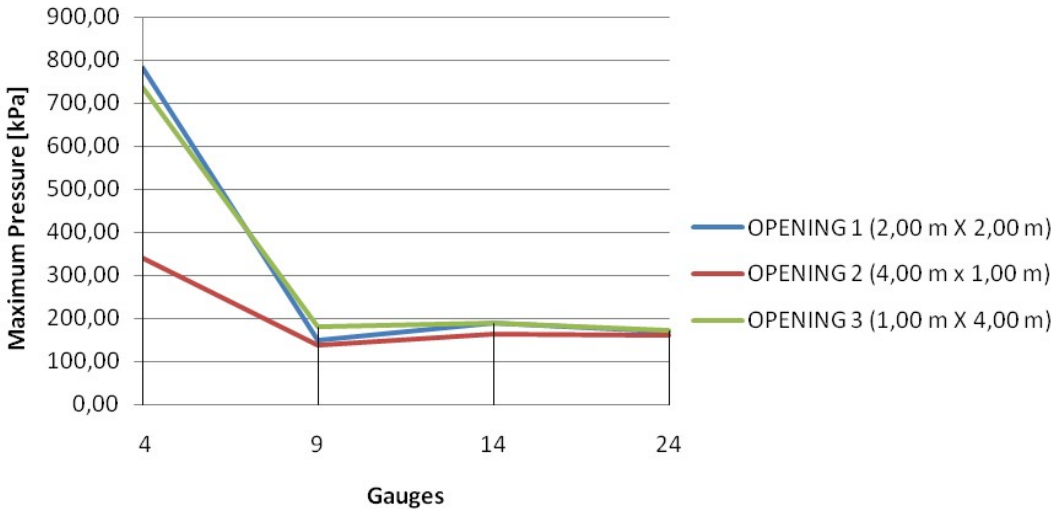

Figure 12: Maximum pressures. 50 kg of TNT, $Z = 0.50$ m/kg$^{1/3}$

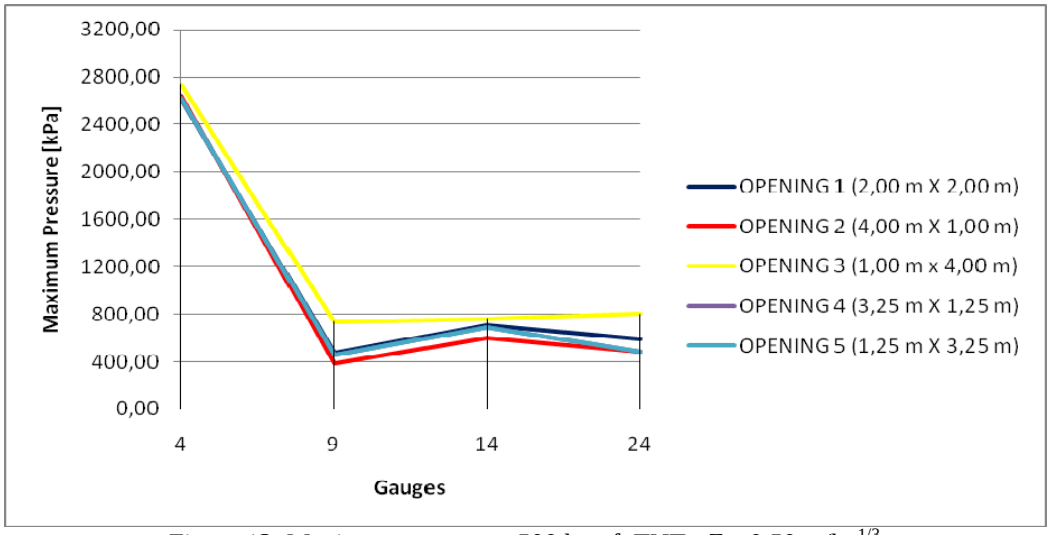

Figure 13: Maximum pressures. 500 kg of TNT, $Z = 0.50$ m/kg$^{1/3}$

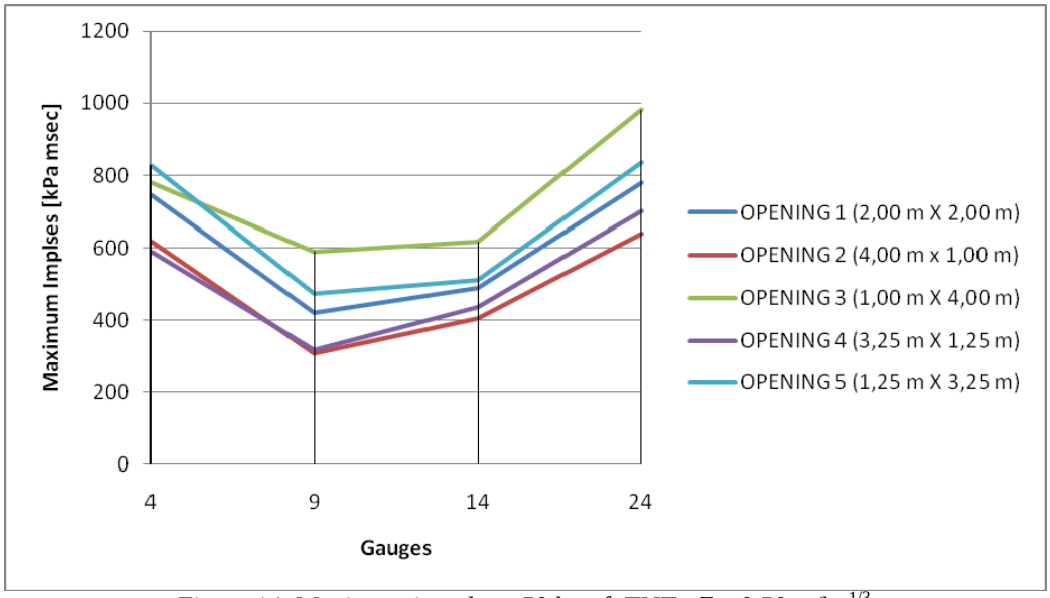

Figure 14: Maximum impulses. 50 kg of TNT, $Z = 0.50$ m/kg$^{1/3}$

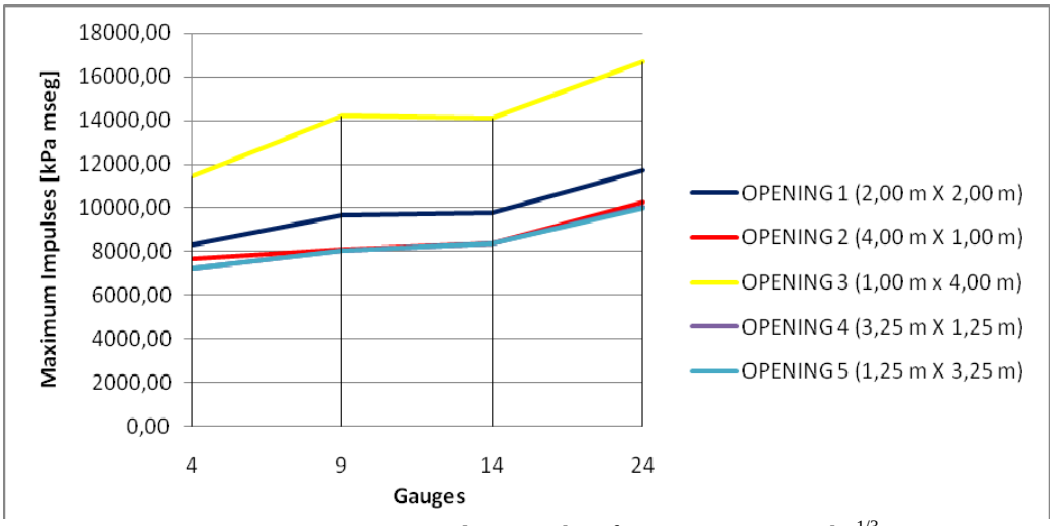

Figure 15: Maximum impulses. 500 kg of TNT, $Z = 0.50$ m/kg$^{1/3}$

6 CONCLUSIONS

A numerical study about the influence of different shapes of windows on the pressures and impulses inside a building subjected to a external blast loading is presented in this paper. The charge consists of 50 and 500 Kg of TNT located at four different locations. The values obtained are important data for the design of structures subjected to explosive charges and a better quantification of the effects produced for it.

The peak values of pressure and impulse does not necessarily decrease with the distance from the center of the explosion. This is due to the complicated effects of reflections produced in the interior of the concerned building.

In the analysis of the five opening options can be noted that in most cases studied, alternatives 2 and 4 present the lowest values in the two variables under discussion (maximum pressures and impulses), at different checkpoints. These two options correspond to rectangular windows arranged horizontally, which leads to determine one of the most important conclusions. This gives a very important fact to consider in designing structures that can be exposed to possible explosions.

ACKNOWLEDGEMENTS

The financial support of the CONICET (Argentina) and SECYT (National University of Cuyo) is gratefully acknowledged.

REFERENCES

Ambrosini D., B. Luccioni (2010). Craters produced by explosive loads carried on vehicles. *Mecánica Computacional, XXIX*:115-131, 2010.

Ambrosini D., B. Luccioni (2009). Reinforced concrete wall as protection against accidental explosions in the petrochemical industry. *Structural Engineering and Mechanics*. Vol. 32 Issue 2, pp 213-234, May 2009.

Baker, W.E., Cox, P.A., Westine, P.S., Kulesz, J.J., & Strehlow, R.A. (1983). *Explosion hazards and evaluation.* Amsterdam: Elsevier.

Batra R.C. and N.M. Hassan (2008). Blast resistance of unidirectional fiber reinforced composites. *Composites Part B: Engineering*. 39(3), 513-536.

Børvik T., A.G. Hanssen, S. Dey, H. Langberg, M. Langseth (2008a). On the ballistic and blast load response of a 20 ft ISO container protected with aluminium panels filled with a local mass—Phase I: Design of protective system. *Engineering Structures* 30, 1605–1620.

Børvik T., A. Burbach, H. Langberg, M. Langseth (2008b). On the ballistic and blast load response of a 20 ft ISO container protected with aluminium panels filled with a local mass—Phase II: Validation of protective system. *Engineering Structures* 30, 1621–1631.

Coughlin A.M., Musselman E.S., Schokker A.J., Linzell D.G. (2010). Behavior of portable fiber reinforced concrete vehicle barriers subject to blasts from contact charges. *International Journal of Impact Engineering.* 37 (2010) 521–529.

Dharmasena K, H Wadley, Z Xue and J Hutchinson (2008). Mechanical response of metallic honeycomb sandwich panel structures to high-intensity dynamic loading. *Int. J. of Impact Engineering*. 35(9), 1063-1074.

Elliot C.L., Mays G.C. and Smith P.D. "The protection of buildings against terrorism and disorder". *Proceedings of Institution of Civil Engineers: Structures & Buildings*, 94, 287-297 (1992).

Jacinto, A., Ambrosini, R.D. Danesi, R. (2001). Experimental and computational analysis of plates under air blast loading, *International J. of Impact Engineering*, 25(10), 927-947.

Jacob N, GN Nurick and GS Langdon (2007). The effect of stand-off distance on the failure of fully clamped circular mild steel plates subjected to blast loads. *Engineering Structures*. 29(10), 2723-2736.

Jones J., Wu C., Oehlers D.J., Whittaker A.S., Sun W., Marks S., Coppola R. (2009). Finite difference analysis of simply supported RC slabs for blast loadings. *Engineering Structures.* 31 (2009) 2825-2832

Kinney GF, Graham KJ (1985). *Explosive shocks in air*. 2nd Edition, Springer Verlag, Berlin.

Lee, E. L., Tarver, C. M. (1980). Phenomenological Model of Shock Initiation in Heterogeneous Explosives. *Physics of Fluids*, 23 (12), 2362-2372 1980.

Lu Y and K Xu (2007). Prediction of debris launch velocity of vented concrete structures under internal blast. *International Journal of Impact Engineering*. 34(11), 1753-1767.

Luccioni B., D. Ambrosini, R. Danesi (2006). Blast Load Assessment using Hydrocodes, *Engineering Structures*, 28(12), 1736-1744.

Luccioni B., Luege M. (2006). Concrete pavement slab under blast loads, *International Journal of Impact Engineering* 32 (2006) 1248–1266.

Main JA and GA Gazonas (2008). Uniaxial crushing of sandwich plates under air blast: Influence of mass distribution. *International Journal of Solids and Structures*. 45(7-8), 2297-2321.

McKown S, Y Shen, W Brookes, C Sutcliffe, W Cantwell, G Langdon, G Nurick and M Theobald (2008). The quasi-static and blast loading response of lattice structures. *Int. J. of Impact Engineering*. 35(8), 795-810.

Raftoyiannis IG., C. Spyrakos, and G.T. Michaltsos (2007). Behavior of suspended roofs under blast loading. *Engineering Structures.* 29(1), 88-100.

Remennikov Alex M., and Timothy A. Rose (2007). Predicting the effectiveness of blast wall barriers using neural network. *International Journal of Impact Engineering*. 34(12), 1907-1923

Schenker A, I Anteby, E Gal, Y Kivity, E Nizri, O Sadot, R Michaelis, O Levintant, and Gabi Ben-Dor (2008). Full-scale field tests of concrete slabs subjected to blast loads. *Int. J. of Impact Engineering*. 35(3), 184-198.

Scherbatiuk K and N Rattanawangcharoen (2008). Experimental testing and numerical modeling of soil-filled concertainer walls. *Engineering Structures*. In Press

Shi Y, H Hao and Z-X Li (2008). Numerical derivation of pressure–impulse diagrams for prediction of RC column damage to blast loads. *International Journal of Impact Engineering.* 35(11), 1213-1227.

Smith P.D., J.G. Hetherington (1994), Blast and Ballistic Loading of Structures, Butterworth-Heinemann Ltd.

Smith P.D., Rose T.A., (2002), Blast loading and building robustness, *Progress in Structural Engineering and Materials*. 4(2), 213-223.

Tekalur SA, AE Bogdanovich and A Shukla (2008). Shock loading response of sandwich panels with 3-D woven E-glass composite skins and stitched foam core. *Composites Science and Technology.*

Wharton RK, Formby SA, Merrifield R (2000). Air-blast TNT equivalence for a range of commercial blasting explosives. *Journal of Hazardous Materials*, A79, 31–39, 2000

Yang G and T-S Lok (2007). Analysis of RC structures subjected to air-blast loading accounting for strain rate effect of steel reinforcement. *International Journal of Impact Engineering.* 34(12), 1924-1935.

Zhou XQ and H Hao (2008). Prediction of airblast loads on structures behind a protective barrier. *International Journal of Impact Engineering.* 35(5), 363-375.